Continuous attractor network models of grid cell firing based on excitatory-inhibitory interactions

Continuous attractor network models of grid cell firing based on excitatory-inhibitory interactions

Oliver Shipston-Sharman [1], Lukas Solanka [1], Matthew F. Nolan [1]

[1] Centre for Integrative Physiology, University of Edinburgh, Hugh Robson Building, Edinburgh, EH8 9XD, United Kingdom

Corresponding author:
Matthew F. Nolan
Centre for Integrative Physiology, University of Edinburgh, Hugh Robson Building, Edinburgh, EH8 9XD, United Kingdom
+44 131 650 9874
mattnolan@ed.ac.uk

Keywords: Gamma oscillation, recurrent network, neural computation, excitation, inhibition, epilepsy

Key points summary:

1. Neurons with grid firing fields are thought to encode estimates of location computed from self-motion signals.

2. Evidence points towards continuous attractor networks as a substrate for grid firing, but the cellular mechanisms are not well understood.

3. Computational models of excitatory and inhibitory cells with realistic membrane dynamics account for grid firing and related network oscillations.

4. We argue that investigation of predictions from models of this kind will be essential to establish mechanisms for grid firing and other cognitive computations.

Abstract

Neurons in the medial entorhinal cortex encode location through spatial firing fields that have a grid-like organisation. The challenge of identifying mechanisms for grid firing has been addressed through experimental and theoretical investigations of medial entorhinal circuits. Here, we discuss evidence for continuous attractor network models that account for grid firing by synaptic interactions between excitatory and inhibitory cells. These models assume that grid-like firing patterns are the result of computation of location from velocity inputs, with additional spatial input required to oppose drift in the attractor state. We focus on properties of continuous attractor networks that are revealed by explicitly considering excitatory and inhibitory neurons, their connectivity and their membrane potential dynamics. Models at this level of detail can account for theta-nested gamma oscillations as well as grid firing, predict spatial firing of interneurons as well as excitatory cells, show how gamma oscillations can be modulated independently from spatial computations, reveal critical roles for neuronal noise, and demonstrate that only a subset of excitatory cells in a network need have grid-like firing fields. Evaluating experimental data against predictions from detailed network models will be important for establishing the mechanisms mediating grid firing.

Abbreviations: MEC, medial entorhinal cortex; L2SCs, layer 2 stellate cells; L2PCs, layer 2 pyramidal cells; E-I, excitatory-inhibitory; PV, parvalbumin.

Introduction

Neural representations of space within the hippocampus and medial entorhinal cortex (MEC) are critical for navigation and memory. Grid cells in the MEC have firing fields that encode position using an allocentric, regular triangular matrix or *grid*-like firing pattern (Hafting et al., 2005). Grid representations have the properties of a high capacity, high resolution and error correcting code for self-localisation (Fiete et al., 2008; Mathis et al., 2012; Sreenivasan and Fiete, 2011). The spatially periodic features of grid firing fields have led to the view that they are the output of computation by a path integrator that translates self-motion signals into estimates of location (McNaughton et al., 2006). In this review, we will consider evidence that network attractor dynamics arising from excitatory-inhibitory interactions account for grid firing patterns within MEC circuits.

The organisation within the MEC of spatial firing properties is an important constraint on mechanistic models for grid firing. Grid cells form networks in anatomically overlapping but functionally discrete modules, with cells of the same module sharing their grid spacing and orientation but having randomly distributed phases (relative offset of grid apices) (Barry et al., 2007; Hafting et al., 2005; Stensola et al., 2012). The highest density of grid cells is in layer 2 of the MEC (Sargolini et al., 2006). Grid cells in this layer also show the greatest prospective bias in their code for location (Kropff et al., 2015). There are two major populations of excitatory cells in this layer. Neurons positive for the marker reelin have stellate morphology and project to the dentate gyrus of the hippocampus (Klink and Alonso, 1997; Varga et al., 2010), while neurons positive for calbindin have a more pyramidal morphology and project to the CA1 region of the hippocampus (Kitamura et al., 2014; Ray et al., 2014; Varga et al., 2010). We will refer to these cell populations as layer 2 stellate cells (L2SCs) and layer 2 pyramidal cells (L2PCs) respectively (Klink and Alonso, 1997)(L2SCs and L2PCs have also been referred to as ‘Ocean’ and ‘Island’ cells (Kitamura et al., 2014)). Both L2SCs and L2PCs may have grid firing fields, although the majority of neurons in each population do not appear to generate typical grid firing patterns (Sun et al., 2015; Tang et al., 2014). During behaviours that produce grid firing, neurons in superficial layers of the

MEC also generate fast gamma frequency (60-140 Hz) oscillations that are modulated by the slower theta rhythm (Chrobak and Buzsaki, 1998; Colgin et al., 2009). While all grid cells encode location through their firing rate, some also represent location through timing of their action potentials relative to the network theta rhythm (Hafting et al., 2008; Reifenstein et al., 2012).

Several conceptual models have been proposed to explain grid firing patterns (for reviews see (Burgess and O'Keefe, 2011; Giocomo et al., 2011; Zilli, 2012)). However, implementing models in ways that are consistent with the biophysics and connectivity of entorhinal neurons is challenging (Pastoll et al., 2012; Remme et al., 2010). Here, we will explore insights from models in which grid-like firing patterns emerge as a result of path integration in continuous attractor networks composed of excitatory and inhibitory neurons, with membrane potential dynamics that approximate real neurons (Figure 1). We will argue that this class of models is particularly useful as they can be constrained by experimentally measured synaptic connectivity and oscillatory network activity, as well as by action potential firing during spatial behaviours. They therefore generate specific predictions that are testable by diverse experimental approaches from anatomical analysis through to electrophysiological recordings of single cell and network activity.

Continuous attractors networks as models for grid generation

Continuous attractor networks are dynamical systems whose intrinsic properties drive activity towards a stable state; this can be visualised in a state space comprising an energy surface upon which stable states are represented by low energy regions (Brody et al., 2003). States existing outwith these regions will decay ‘downwards’ towards the low energy points. A network’s intrinsic connections can be configured so its preferred states will correspond to localised bumps of activity. Mathematical functions can then be implemented in the network’s state space by movement of the bumps of activity in response to inputs to the network (Conklin and Eliasmith, 2005; Eliasmith, 2005). In continuous attractor network models of spatial coding, the

computation performed is integration of velocity input to generate an estimate of location relative to a known start point, referred to as path integration (McNaughton et al., 1996; McNaughton et al., 2006; Samsonovich and McNaughton, 1997; Zhang, 1996). Such networks do not necessarily generate triangular grid-like firing fields, but can do so with appropriately configured connections. In networks that model grid firing, stable states manifest either as a bump (Figure 2A) or as multiple bumps of activity (Figure 2B) on a two-dimensional sheet of phase-arranged grid cells (Fuhs and Touretzky, 2006; Guanella et al., 2007). Given velocity inputs the activity bump(s) represent movement in space by propagating across the sheet. This mechanism for path integration can be implemented by networks in which individual grid cells receive velocity inputs tuned to a particular movement direction, with the local connections of each grid cell offset so that an increase in its input will tend to push the activity bump in an appropriate direction across the neural sheet (Burak and Fiete, 2009; Fuhs and Touretzky, 2006; Guanella et al., 2007). Alternatively, path integration could be achieved through interactions between a layer of heading-independent grid cells and multiple layers of head direction-modulated grid cells, which each integrate a single head direction input with speed signals and feedback from the heading-independent grid layer (Samsonovich and McNaughton, 1997). While the latter class of models require many more neurons to account for path integration, because separate layers are required for each heading direction, they have the advantage that they naturally account for direction modulated (or conjunctive) grid cells as well as pure grid cells.

Continuous attractor network models have been implemented at various levels of detail and a close correspondence to known neural connectivity or dynamics is not necessary to generate grid-like firing fields. Indeed, experimental observations have corroborated a number of generic predictions that are independent of the details of the circuitry used for model implementation (McNaughton et al., 2006). 1. Populations of grid cells are organised into modules in which each neuron has a common spatial phase and orientation (Stensola et al., 2012). 2. The spatial phase relationship between cells is maintained even following environmental manipulations that

restructure the spatial firing pattern of individual cells (Yoon et al., 2013). 3. The envelope of the membrane potential of grid cells changes slowly on entry to and exit from their firing fields (Domnisoru et al., 2013; Schmidt-Hieber and Hausser, 2013). 4. Removal of excitatory drive causes cells that previously had grid fields to encode head direction (Bonnevie et al., 2013), which is consistent with movement of activity bumps in continuous attractor networks relying on each grid cell receiving a tuned head direction input (Bonnevie et al., 2013; Burak and Fiete, 2009; Fuhs and Touretzky, 2006; Guanella et al., 2007; Pastoll et al., 2013).

While these observations are consistent with continuous attractor network models accounting for rate coded grid fields, most existing models do not readily account for precession in the timing of action potentials fired by some grid cells relative to the theta rhythm (Hafting et al., 2008; Reifenstein et al., 2012). One-dimensional attractor networks, based on interaction between a direction-independent cell population and direction modulated cell populations, can generate repeating firing fields and phase precession (Navratilova et al., 2012). Extension of this mechanism to two dimensions will require additional neuronal layers for each heading direction (Samsonovich and McNaughton, 1997). An alternative is that phase precession and attractor states are established independently. For example, phase precession can be explained by hybrid models that include a mechanism for grid firing based on interference between oscillations (Burgess et al., 2007; Hasselmo et al., 2007), in addition to mechanisms for generation of network attractor states (Bush and Burgess, 2014; Schmidt-Hieber and Hausser, 2013).

Emergence of attractor states through excitatory-inhibitory interactions

How might attractor mechanisms for grid firing be implemented in networks of neurons? Do the properties of neural circuitry in the MEC constrain models or lead to predictions that distinguish between different models? Grid computation in continuous attractor networks requires emergence of stable bumps of activity. This can be achieved using reduced models in which separate populations of excitatory and inhibitory neurons are not explicitly considered. In these models, either each neuron locally excites nearby

neurons and inhibits more distant neurons (Fuhs and Touretzky, 2006), or spatially structured inhibitory connections act in concert with excitatory drive to the whole network (Burak and Fiete, 2009; Couey et al., 2013). However, use of local excitatory connections is inconsistent with evidence that L2SCs are not directly connected to one another (Dhillon and Jones, 2000; Pastoll et al., 2013; Couey et al., 2013), but instead interact indirectly via inhibitory interneurons (Pastoll et al., 2013; Couey et al., 2013). Moreover, because grid cells are excitatory neurons, an inhibitory output from grid cells is inevitably an over-simplification. One could address this by assuming that the inhibitory output from grid cells is equivalent to an excitatory connection to a dedicated inhibitory interneuron. However, this is inconsistent with convergent (many to one) and divergent (one to many) connectivity between excitatory and inhibitory networks (Couey et al., 2013), and with there being many more excitatory than inhibitory neurons in layer 2 of the MEC (Canto et al. 2008). Thus, while offering conceptually important explanations for grid firing, reduced models are limited in their ability to evaluate consequences of experimentally determined connectivity.

Models that explicitly consider interactions between separate populations of excitatory and inhibitory neurons inevitably differ from reduced models, leading to new insights and predictions (Pastoll et al., 2013; Solanka et al., 2015; Widloski and Fiete, 2014). Given appropriately structured network connectivity these excitatory-inhibitory (E-I) models generate network attractor states (Figure 2). Structured connectivity can be implemented by varying the strength of connections between neurons according to their position in the network, while maintaining a fixed probability of a connection being present (Pastoll et al., 2013; Solanka et al., 2015; Widloski and Fiete, 2014). Alternatively, synaptic strength can remain fixed but the probability of connections varied as a function of distance between pre- and postsynaptic neurons on the neural sheet (Solanka et al., 2015). Evidence that the amplitude of inhibitory inputs to stellate cells has a bimodal distribution is consistent with structuring of connection probability rather than the strength of connections (Couey et al 2013). Models based on E-I interactions also demonstrate that velocity inputs, which are required for movement-dependent

translation of their activity bumps, may target either interneurons or excitatory cells (Pastoll et al. 2013). While spatial firing of cells with inhibitory output is implicit in reduced models, in E-I models interneurons have spatial firing fields that depend on the wiring of the network. For example, either surround inhibition or surround excitation supports grid firing by excitatory cells, but in the latter case interneurons have inverted grid fields, whereas in the former they have grid-like fields (Pastoll et al. 2013).

Two important recent experimental studies introduce challenges beyond simply accounting for grid firing by excitatory cells. First, while the firing fields of parvalbumin (PV) positive interneurons have significant spatial stability, they typically have grid scores below the threshold for grid firing, only rarely appear to have a clear grid like organisation (Buetfering et al. 2014), and on visual inspection also do not appear to have inverted firing fields although this is difficult to establish quantitatively. Second, when layer 2 cells are imaged in freely moving animals, only about 10 % of identified L2SCs and L2PCs have grid-like firing fields (Sun et al., 2015). This is surprising given that neurons within each population appear to have similar synaptic connectivity and intrinsic properties. This could suggest that the grid firing neurons correspond to sub-groups of cells with distinct, but not yet identified, cellular or circuit properties. Otherwise, models for grid firing must explain how grid patterns are produced by only a subset of neurons that at a cellular and circuit level are indistinguishable from non-grid cells.

These challenges may be addressed using E-I networks and by considering that in vivo entorhinal neurons may receive spatial signals that can be considered as noise in the sense that they are not used to promote grid firing. Thus, when E-I models are extended to include random spatial input to interneurons, excitatory neurons in these networks continue to generate grid-like firing fields, but the hexagonal symmetry of interneuron firing fields is reduced (Figure 3)(Solanka et al. 2015). In these networks the fraction of excitatory and inhibitory cells classified as grid cells drops substantially, with almost no interneurons classified as having grid fields (Figure 3). Thus, the finding that only a subset of layer 2 cells have grid-like firing fields need not

imply that grid and non-grid cells are distinguished by distinct cellular or circuit properties, while the absence of a clear grid signature in the firing of individual interneurons may nevertheless be compatible with models based on E-I interactions.

Single and multi-bump networks differ in their local and long-range connectivity

Continuous attractor network models for grid firing exist in versions that differ in their number of activity bumps. These functional differences result primarily from connections spanning different distances relative to the size of the network.

In single bump networks (also referred to as periodic networks, cf. Widlowski and Fiete, 2015) the planar attractor manifold is wrapped into a torus (Guanella et al., 2007; Pastoll et al., 2013; Samsonovich and McNaughton, 1997). This conceptual torus structure is actuated in the synaptic connectivity of the network, with cells on one edge of the sheet connected to those on the opposite side (Figure 2A). When an animal travels continuously in one direction the activity bump moves periodically around the network. Generation of a triangular rather than rectangular organisation of grid fields is dependant on the addition of a phase shift in one axis resulting in a twisted torus attractor manifold (Figure 2A).

Networks with multiple bumps of activity also have their neurons arranged on a two dimensional manifold, however, a hexagonal population activity bump organisation arises from the most energetically efficient packing of the rings of inhibition; each circle of inhibition repels neighbouring circles to a maximal distance until stabilising into a grid of activity bumps (Figure 2B)(Burak and Fiete, 2009; Couey et al., 2013; Fuhs and Touretzky, 2006). During movement the bumps of activity propagate across the network and individual neurons generate grid firing patterns. Multi-bump networks can either be implemented with periodic boundaries (also referred to as partially periodic networks), so that much as in single bump models the activity bump wraps to the other side of the network. Alternatively, they can have boundaries (also

297 referred to as aperiodic networks). In this case, when bumps reach the edge
298 of the network they disappear, while on the opposite side of the network local
299 competitive synaptic interactions cause new bumps to spontaneously form as
300 existing bumps move away (Burak and Fiete, 2009; Fuhs and Touretzky,
301 2006).
302
303 When single bump attractors are implemented in E-I networks, each neuron's
304 connections extend over a relatively large fraction of the network (Figure 2A).
305 Thus, neurons making surround connections have their highest connection
306 probability, or connection strength, with neurons at a distance of
307 approximately half the width of the untwisted neural sheet. This distance
308 refers to separation based on the order of connectivity in the network rather
309 than anatomical distance (cf. (Widloski and Fiete, 2014)). Indeed the
310 anatomical organisation of cell bodies of neurons with repeating firing fields
311 appears relatively weak compared to the organisation of neural sheets in
312 continuous attractor network models (Heys et al., 2014), suggesting that
313 synaptic connectivity required for grid firing can be established without
314 ordering of neuronal cell bodies (Widloski and Fiete, 2014). In contrast to
315 single bump networks, the connectivity in multi-bump attractors is much more
316 localised relative to the overall size of the network (Figure 2B). This suggests
317 that quantification of the extent of connectivity between excitatory and
318 inhibitory neurons could be used to distinguish between single and multi-
319 bump models. Local circuit perturbations through thermo- or chemo-
320 modulation in conjunction with multi-unit recordings might also distinguish
321 between single and multi-bump networks (Widloski and Fiete, 2015).
322
323 **Excitatory-inhibitory interactions provide a common mechanism for grid**
324 **firing and network oscillations**
325 Successful models of brain circuits should account for network dynamics as
326 well as the firing patterns of individual cells. Dynamics can be modelled by
327 simulating networks of integrate and fire neurons. In these models synaptic
328 input to a neuron charges its membrane capacitance, which is in turn
329 discharged through a resistance. Action potentials occur when the membrane
330 potential crosses a threshold. In exponential integrate and fire neurons the

spike threshold has been replaced with an exponential function in order to obtain more realistic spike initiation dynamics (Fourcaud-Trocme et al., 2003). Although integrate and fire models neglect details of morphology and ion channel biophysics, their dynamics are a good approximation for physiological synaptic integration, making them an important bridge between abstract theoretical and more detailed cellular models.

Models of interacting populations of excitatory and inhibitory exponential integrate and fire neurons can account for both grid firing and gamma oscillations (Pastoll et al. 2013, Solanka et al. 2015). When the models receive theta modulated input the gamma oscillations are nested at a fixed phase within each theta cycle (Figure 4). This is consistent with experimental findings that theta modulated optogenetic activation of layer 2 circuits is sufficient to generate nested gamma activity resembling that observed in behaving animals (Pastoll et al. 2013, Chrobak et al. 2000). In these experiments, and in the corresponding models, gamma oscillations emerge through fast time scale E-I interactions. On each gamma cycle a subset of excitatory neurons fire action potentials. Because the output from each excitatory neurons diverges to many interneurons (Figure 2A), and as each interneuron receives convergent input from many excitatory cells (Figure 2A), this output is sufficient to rapidly trigger action potentials in a large fraction of interneurons. Divergent projections from interneurons send inhibitory feedback to excitatory cells, including those that did not spike. A second gamma cycle is initiated on recovery from this inhibition. The divergent connectivity effectively implements a competitive mechanism that limits the number of excitatory cells active on each theta cycle (Tiesinga and Sejnowski, 2009). While E-I models account for both rate coded firing and nested gamma oscillations, a possible limitation of existing models is that theta input is implemented as a common drive to E and I cells. In contrast, only interneurons in the MEC appear to receive inhibitory pacemaker input from the medial septum (Gonzalez-Sulser et al., 2014) while the origin of excitation during theta is currently unknown.

Models that account for grid firing and nested gamma oscillations exclusively through E-I interactions have been extended to incorporate additional features of MEC circuitry (Solanka et al. 2015). Experimental observations indicate that inhibitory neurons in layer 2 of the MEC may synapse with one another (Pastoll et al. 2013). Addition to E-I models of connections between interneurons stabilises grid firing and increases the frequency of nested gamma oscillations (Solanka et al. 2015). The resulting E-I-I models more easily produce theta oscillations with frequency that matches that of gamma activity in vivo (cf. Chrobak et al. 1998, Colgin et al. 2012). Although E-I models were initially motivated by the indirect connectivity between L2SCs, grid cells are found in deeper layers in which excitatory cells are likely to communicate directly with one another (Dhillon and Jones, 2000). Moreover, while many models for grid firing have focussed on L2SCs, L2PCs also have grid firing fields (Sun et al., 2015), and the synaptic mechanisms through which they interact may differ. When E-I models are extended to include structured connectivity between excitatory neurons in addition to structured E-I interactions they continue to generate grid firing patterns (Widloski and Fiete, 2014) and nested gamma oscillations (Solanka et al. 2015). However, when these models were modified further so that inhibitory connectivity is random and only excitatory connectivity is structured they were unable to generate stable grid firing fields (Solanka et al. 2015). We suspect this results from requirements for precise tuning of connections in continuous attractor networks based on structured excitation (cf. (Seung et al., 2000)).

The strong theta frequency modulation of activity in the MEC raises the question of how attractor states might be maintained during phases of the theta cycle in which activity is suppressed. In principle if activity is suppressed for a sufficient duration then when activity resumes the network has no memory of the location of the previous bump. The spatial representation necessary for path integration is then lost. This loss of bump stability can be prevented by synaptic or intrinsic conductances with slow dynamics (Navratilova et al., 2012; Pastoll et al., 2013; Solanka et al., 2015). For example, on the start of each new theta cycle the residual excitatory NMDA receptor current ensures bumps re-form in their previous location (Figure 4).

While there is evidence that NMDA receptors in entorhinal interneurons have sufficiently slow kinetics to perform this role (Jones and Buhl, 1993), it is possible that other biophysical processes that have slow dynamics such as intracellular Ca^{2+} signalling or kinetics of the action potential afterhyperpolarisation could also stabilise attractor states across theta cycles (Navratilova et al., 2012). Alternatively, theta modulation may not completely inactivate entorhinal networks, in which case bump location could be maintained through neurons that remain active across the full theta cycle. Further experimental testing of these ideas will require a better understanding of cellular mechanisms underlying modulation of entorhinal activity during theta states.

Noise enables independent control of theta nested gamma oscillations and grid firing by modulation of excitatory-inhibitory interactions

Because E-I models account for rate coded grid computation and gamma frequency network activity, they provide an opportunity to investigate relationships between these phenomena. Many cognitive functions, in addition to spatial computation by grid networks, are associated with modulation of gamma activity (Uhlhaas and Singer, 2012). In turn, both cognitive function and gamma activity correlate with changes in E-I interactions. However, the causal relationships between the strength of excitatory and inhibitory synapses, gamma oscillations and computations that might underlie key cognitive functions have been difficult to establish. Systematic investigation of E-I models suggests that these relationships are complex (Solanka et al. 2015). First, nested gamma oscillations and grid firing are both promoted by an optimal level of noise within a network. If noise is too low seizure-like states that suppress grid firing tend to emerge, whereas if noise is too high grid fields drift and gamma becomes less coherent. Second, intermediate noise levels maximise the range of excitatory and inhibitory synaptic strengths that support grid firing. Third, gamma activity is a poor predictor of grid firing. Thus, varying the strength of inhibitory or excitatory connections can tune the frequency and power of gamma oscillations without affecting grid firing. Fourth, tuning of intrinsic connections could be used to modulate oscillation-based codes while maintaining grid firing, for example to determine the

response of downstream neurons to convergent input from different grid modules. Thus, synchronisation of gamma activity between grid modules might promote, and discordant tuning of gamma between modules might oppose, downstream integration. Therefore, the potential for independent control of gamma oscillations and grid firing, even though both phenomena arise from a common circuit mechanism, has implications for physiological and pathological states of MEC circuits.

Conclusion

Because multiple abstract models are able to produce grid-like periodic spatial firing patterns, additional experimental constraints are required to establish mechanisms used by the brain to generate grid firing. We have considered evidence that continuous attractor networks that use velocity inputs to compute grid codes for location can be implemented through E-I interactions that are consistent with known properties of microcircuits in the MEC. When implemented with realistic neuronal dynamics these models also account for theta nested gamma oscillations, although so far they are unable to explain theta phase precession in two dimensions without incorporation of additional mechanisms for path integration. Critical future tests of continuous attractor network hypotheses for grid firing include evaluation of predictions for the firing patterns and connectivity of excitatory and inhibitory cell populations. E-I models make further assumptions concerning integration of velocity signals (Pastoll et al. 2013), error correction by place and border input (Guanella et al., 2007; Hardcastle et al., 2015; Pastoll et al., 2013; Sreenivasan and Fiete, 2011) and sources of tonic drive (Bonnevie et al., 2013; Burak and Fiete, 2009; Pastoll et al., 2013) that we have not considered here. Experimental evidence for how these signals are integrated by MEC circuits will further constrain possible models. Progress in establishing experimentally constrained models for spatial representation by cell populations in the MEC may serve as a proof of principle for understanding cellular and synaptic mechanisms for high-level computations by cortical circuits in general.

References

Barry, C., Hayman, R., Burgess, N., and Jeffery, K.J. (2007). Experience-dependent rescaling of entorhinal grids. Nat Neurosci *10*, 682-684.

Bonnevie, T., Dunn, B., Fyhn, M., Hafting, T., Derdikman, D., Kubie, J.L., Roudi, Y., Moser, E.I., and Moser, M.B. (2013). Grid cells require excitatory drive from the hippocampus. Nat Neurosci *16*, 309-317.

Brody, C.D., Romo, R., and Kepecs, A. (2003). Basic mechanisms for graded persistent activity: discrete attractors, continuous attractors, and dynamic representations. Curr Opin Neurobiol *13*, 204-211.

Burak, Y., and Fiete, I.R. (2009). Accurate path integration in continuous attractor network models of grid cells. PLoS Comput Biol *5*, e1000291.

Burgess, N., Barry, C., and O'Keefe, J. (2007). An oscillatory interference model of grid cell firing. Hippocampus *17*, 801-812.

Burgess, N., and O'Keefe, J. (2011). Models of place and grid cell firing and theta rhythmicity. Curr Opin Neurobiol.

Bush, D., and Burgess, N. (2014). A hybrid oscillatory interference/continuous attractor network model of grid cell firing. J Neurosci *34*, 5065-5079.

Chrobak, J.J., and Buzsaki, G. (1998). Gamma oscillations in the entorhinal cortex of the freely behaving rat. J Neurosci *18*, 388-398.

Colgin, L.L., Denninger, T., Fyhn, M., Hafting, T., Bonnevie, T., Jensen, O., Moser, M.B., and Moser, E.I. (2009). Frequency of gamma oscillations routes flow of information in the hippocampus. Nature *462*, 353-357.

Conklin, J., and Eliasmith, C. (2005). A controlled attractor network model of path integration in the rat. J Comput Neurosci *18*, 183-203.

Couey, J.J., Witoelar, A., Zhang, S.J., Zheng, K., Ye, J., Dunn, B., Czajkowski, R., Moser, M.B., Moser, E.I., Roudi, Y.*, et al.* (2013). Recurrent inhibitory circuitry as a mechanism for grid formation. Nat Neurosci *16*, 318-324.

Dhillon, A., and Jones, R.S. (2000). Laminar differences in recurrent excitatory transmission in the rat entorhinal cortex in vitro. Neuroscience *99*, 413-422.

Domnisoru, C., Kinkhabwala, A.A., and Tank, D.W. (2013). Membrane potential dynamics of grid cells. Nature *495*, 199-204.

Eliasmith, C. (2005). A unified approach to building and controlling spiking attractor networks. Neural Comput *17*, 1276-1314.

Fiete, I.R., Burak, Y., and Brookings, T. (2008). What grid cells convey about rat location. J Neurosci *28*, 6858-6871.

Fourcaud-Trocme, N., Hansel, D., van Vreeswijk, C., and Brunel, N. (2003). How spike generation mechanisms determine the neuronal response to fluctuating inputs. J Neurosci *23*, 11628-11640.

Fuhs, M.C., and Touretzky, D.S. (2006). A spin glass model of path integration in rat medial entorhinal cortex. J Neurosci *26*, 4266-4276.

Giocomo, L.M., Moser, M.B., and Moser, E.I. (2011). Computational models of grid cells. Neuron *71*, 589-603.

Gonzalez-Sulser, A., Parthier, D., Candela, A., McClure, C., Pastoll, H., Garden, D., Surmeli, G., and Nolan, M.F. (2014). GABAergic projections from the medial septum selectively inhibit interneurons in the medial entorhinal cortex. J Neurosci *34*, 16739-16743.

513 Guanella, A., Kiper, D., and Verschure, P. (2007). A model of grid cells based on a
514 twisted torus topology. Int J Neural Syst *17*, 231-240.
515 Hafting, T., Fyhn, M., Bonnevie, T., Moser, M.B., and Moser, E.I. (2008).
516 Hippocampus-independent phase precession in entorhinal grid cells. Nature *453*,
517 1248-1252.
518 Hafting, T., Fyhn, M., Molden, S., Moser, M.B., and Moser, E.I. (2005).
519 Microstructure of a spatial map in the entorhinal cortex. Nature *436*, 801-806.
520 Hardcastle, K., Ganguli, S., and Giocomo, L.M. (2015). Environmental boundaries
521 as an error correction mechanism for grid cells. Neuron *86*, 827-839.
522 Hasselmo, M.E., Giocomo, L.M., and Zilli, E.A. (2007). Grid cell firing may arise
523 from interference of theta frequency membrane potential oscillations in single
524 neurons. Hippocampus *17*, 1252-1271.
525 Heys, J.G., Rangarajan, K.V., and Dombeck, D.A. (2014). The functional micro-
526 organization of grid cells revealed by cellular-resolution imaging. Neuron *84*,
527 1079-1090.
528 Jones, R.S., and Buhl, E.H. (1993). Basket-like interneurones in layer II of the
529 entorhinal cortex exhibit a powerful NMDA-mediated synaptic excitation.
530 Neurosci Lett *149*, 35-39.
531 Kitamura, T., Pignatelli, M., Suh, J., Kohara, K., Yoshiki, A., Abe, K., and Tonegawa,
532 S. (2014). Island cells control temporal association memory. Science *343*, 896-
533 901.
534 Klink, R., and Alonso, A. (1997). Morphological characteristics of layer II
535 projection neurons in the rat medial entorhinal cortex. Hippocampus *7*, 571-583.
536 Kropff, E., Carmichael, J.E., Moser, M.B., and Moser, E.I. (2015). Speed cells in the
537 medial entorhinal cortex. Nature *523*, 419-424.
538 Mathis, A., Herz, A.V., and Stemmler, M. (2012). Optimal population codes for
539 space: grid cells outperform place cells. Neural Comput *24*, 2280-2317.
540 McNaughton, B.L., Barnes, C.A., Gerrard, J.L., Gothard, K., Jung, M.W., Knierim, J.J.,
541 Kudrimoti, H., Qin, Y., Skaggs, W.E., Suster, M.*, et al.* (1996). Deciphering the
542 hippocampal polyglot: the hippocampus as a path integration system. J Exp Biol
543 *199*, 173-185.
544 McNaughton, B.L., Battaglia, F.P., Jensen, O., Moser, E.I., and Moser, M.B. (2006).
545 Path integration and the neural basis of the 'cognitive map'. Nat Rev Neurosci *7*,
546 663-678.
547 Navratilova, Z., Giocomo, L.M., Fellous, J.M., Hasselmo, M.E., and McNaughton, B.L.
548 (2012). Phase precession and variable spatial scaling in a periodic attractor map
549 model of medial entorhinal grid cells with realistic after-spike dynamics.
550 Hippocampus *22*, 772-789.
551 Pastoll, H., Ramsden, H.L., and Nolan, M.F. (2012). Intrinsic electrophysiological
552 properties of entorhinal cortex stellate cells and their contribution to grid cell
553 firing fields. Front Neural Circuits *6*, 17.
554 Pastoll, H., Solanka, L., van Rossum, M.C., and Nolan, M.F. (2013). Feedback
555 inhibition enables theta-nested gamma oscillations and grid firing fields. Neuron
556 *77*, 141-154.
557 Ray, S., Naumann, R., Burgalossi, A., Tang, Q., Schmidt, H., and Brecht, M. (2014).
558 Grid-layout and theta-modulation of layer 2 pyramidal neurons in medial
559 entorhinal cortex. Science *343*, 891-896.
560 Reifenstein, E.T., Kempter, R., Schreiber, S., Stemmler, M.B., and Herz, A.V. (2012).
561 Grid cells in rat entorhinal cortex encode physical space with independent firing

562 fields and phase precession at the single-trial level. Proc Natl Acad Sci U S A *109*,
563 6301-6306.
564 Remme, M.W., Lengyel, M., and Gutkin, B.S. (2010). Democracy-independence
565 trade-off in oscillating dendrites and its implications for grid cells. Neuron *66*,
566 429-437.
567 Samsonovich, A., and McNaughton, B.L. (1997). Path integration and cognitive
568 mapping in a continuous attractor neural network model. J Neurosci *17*, 5900-
569 5920.
570 Sargolini, F., Fyhn, M., Hafting, T., McNaughton, B.L., Witter, M.P., Moser, M.B., and
571 Moser, E.I. (2006). Conjunctive representation of position, direction, and velocity
572 in entorhinal cortex. Science *312*, 758-762.
573 Schmidt-Hieber, C., and Hausser, M. (2013). Cellular mechanisms of spatial
574 navigation in the medial entorhinal cortex. Nat Neurosci *16*, 325-331.
575 Seung, H.S., Lee, D.D., Reis, B.Y., and Tank, D.W. (2000). Stability of the memory of
576 eye position in a recurrent network of conductance-based model neurons.
577 Neuron *26*, 259-271.
578 Solanka, L., van Rossum, M.C., and Nolan, M.F. (2015). Noise promotes
579 independent control of gamma oscillations and grid firing within recurrent
580 attractor networks. Elife *4*, e06444.
581 Sreenivasan, S., and Fiete, I. (2011). Grid cells generate an analog error-
582 correcting code for singularly precise neural computation. Nat Neurosci *14*,
583 1330-1337.
584 Stensola, H., Stensola, T., Solstad, T., Froland, K., Moser, M.B., and Moser, E.I.
585 (2012). The entorhinal grid map is discretized. Nature *492*, 72-78.
586 Sun, C., Kitamura, T., Yamamoto, J., Martin, J., Pignatelli, M., Kitch, L.J., Schnitzer,
587 M.J., and Tonegawa, S. (2015). Distinct speed dependence of entorhinal island
588 and ocean cells, including respective grid cells. Proc Natl Acad Sci U S A *112*,
589 9466-9471.
590 Tang, Q., Burgalossi, A., Ebbesen, C.L., Ray, S., Naumann, R., Schmidt, H., Spicher,
591 D., and Brecht, M. (2014). Pyramidal and stellate cell specificity of grid and
592 border representations in layer 2 of medial entorhinal cortex. Neuron *84*, 1191-
593 1197.
594 Tiesinga, P., and Sejnowski, T.J. (2009). Cortical enlightenment: are attentional
595 gamma oscillations driven by ING or PING? Neuron *63*, 727-732.
596 Uhlhaas, P.J., and Singer, W. (2012). Neuronal dynamics and neuropsychiatric
597 disorders: toward a translational paradigm for dysfunctional large-scale
598 networks. Neuron *75*, 963-980.
599 Varga, C., Lee, S.Y., and Soltesz, I. (2010). Target-selective GABAergic control of
600 entorhinal cortex output. Nat Neurosci *13*, 822-824.
601 Widloski, J., and Fiete, I.R. (2014). A Model of Grid Cell Development through
602 Spatial Exploration and Spike Time-Dependent Plasticity. Neuron *83*, 481-495.
603 Widloski, J., and Fiete, I.R. (2015). Cortical microcircuit determination through
604 perturbation and sparse sampling in grid cells. bioRxiv
605 http://dx.doi.org/10.1101/019224.
606 Yoon, K., Buice, M.A., Barry, C., Hayman, R., Burgess, N., and Fiete, I.R. (2013).
607 Specific evidence of low-dimensional continuous attractor dynamics in grid cells.
608 Nat Neurosci *16*, 1077-1084.
609 Zhang, K. (1996). Representation of spatial orientation by the intrinsic dynamics
610 of the head-direction cell ensemble: a theory. J Neurosci *16*, 2112-2126.

611 Zilli, E.A. (2012). Models of grid cell spatial firing published 2005-2011. Front
612 Neural Circuits *6*, 16.
613
614
615 **Additional information**
616
617 Competing interests
618 None of the authors has any conflicts of interest.
619
620 Funding
621 This work was supported by grants to MN from the BBSRC (Bb/L010496/1
622 and Bb/1022147/1).
623
624 Acknowledgements
625 We thank Gulsen Surmeli, Derek Garden and Sarah Tennant for comments
626 on the manuscript.
627

Figure 1. Components of a generic E-I model for generation of grid firing and nested gamma oscillations

Integration of velocity input by continuous attractor networks built from interacting excitatory and inhibitory neurons can generate grid firing fields. When the networks receive a theta modulated input they generate gamma frequency output that is modulated at theta frequency. A spatial input is required to oppose drift in the grid representation. Data are from Pastoll et al. (2013).

Figure 2. Single and multi-bump attractor model of grid firing have distinct circuit organisation

In single bump models grid firing of excitatory cells can be generated by synaptic profiles that produce either surround excitation or surround inhibition. The surround connectivity is strongest for connections to neurons at a distance of about one half the width of the sheet. Each neuron makes divergent connections to many target neurons, and receives convergent input from many pre-synaptic neurons. In multi-bump networks the strongest connections are onto neurons at a much shorter distance relative to the size of the sheet. The upper graphs plot synaptic strength as a function of position in the neural sheet, which is given a width of one. The plots below schematise the resulting E-I connectivity, illustrate the organisation of activity in the neural sheet and the organisation of excitatory cell activity in three dimensions. The connectivity profiles shown for the multi-bump models are based on networks containing only inhibitory neurons, with either surround inhibition (Burak and Fiete, 2009) or local inhibition (Couey et al., 2013). The networks could be considered as having dedicated interneurons receiving input from each excitatory neuron.

Figure 3. Spatial firing of interneurons in E-I attractor models

(A) Schematic organisation of an E-I network with additional random place field inputs to each interneuron (left). Example firing fields of I cells (middle) and E cells (right) are shown adjacent to the schematised neurons. (B)

Histograms of the spatial sparsity (upper) and gridness score (lower) for E-I networks simulated as in (A). Note that most interneurons and many excitatory cells have grid scores < 0.5. Data are from Solanka et al. 2015

Figure 4. Theta nested gamma activity in E-I models

Spike rasters for E cells (red) and I cells (blue) during two theta cycles (grey). The excitatory synaptic input to a representative I cell is illustrated below. Note that a substantial residual inward current (blue shading) is maintained during the phase of the theta oscillation when spike activity of excitatory cells is reduced. The residual current enables the bump of activity to be maintained across theta cycles. Data are from Pastoll et al. (2013) and Solanka et al. (2015).

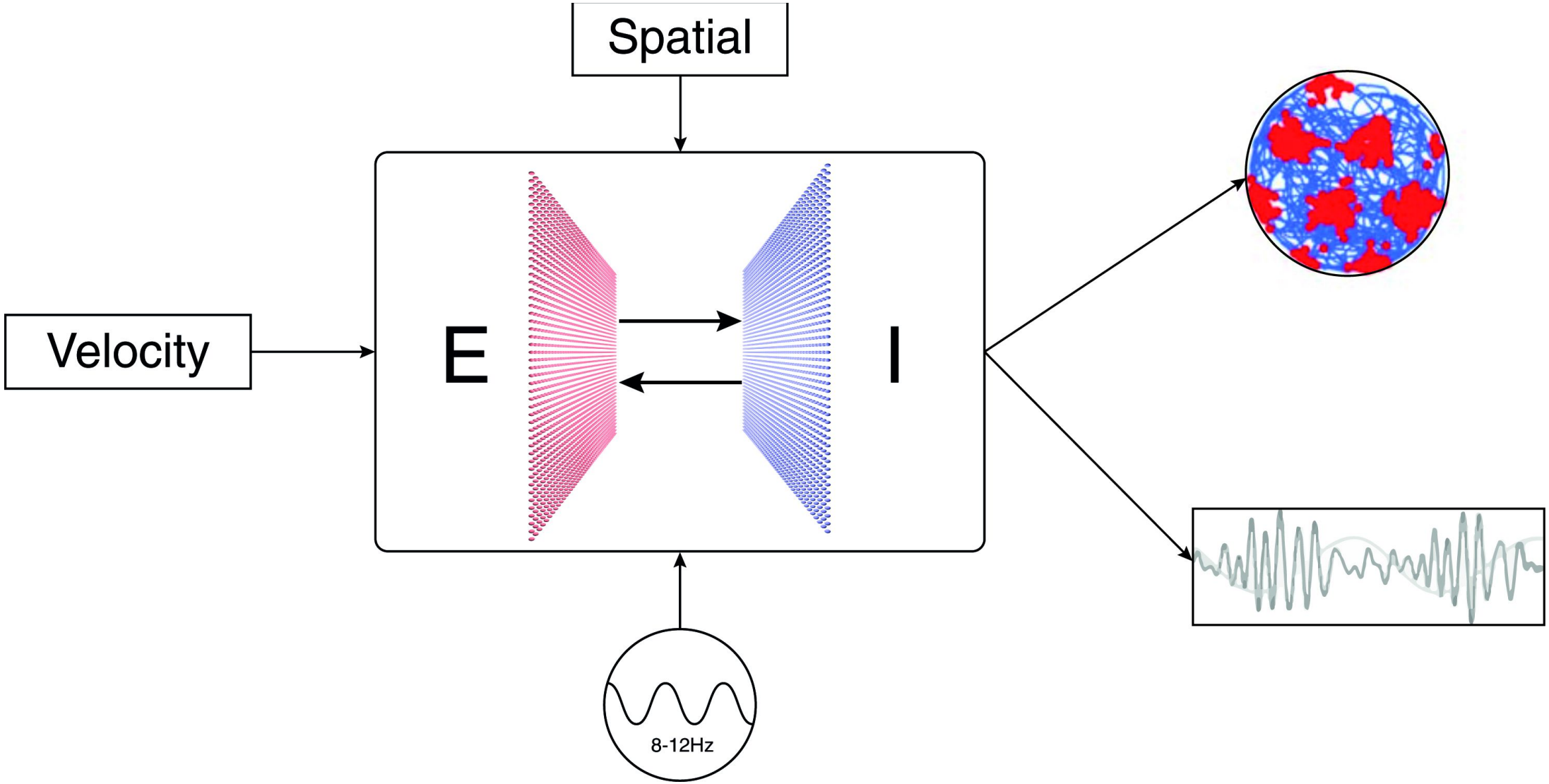
Spatial
Velocity
E
I
8-12Hz

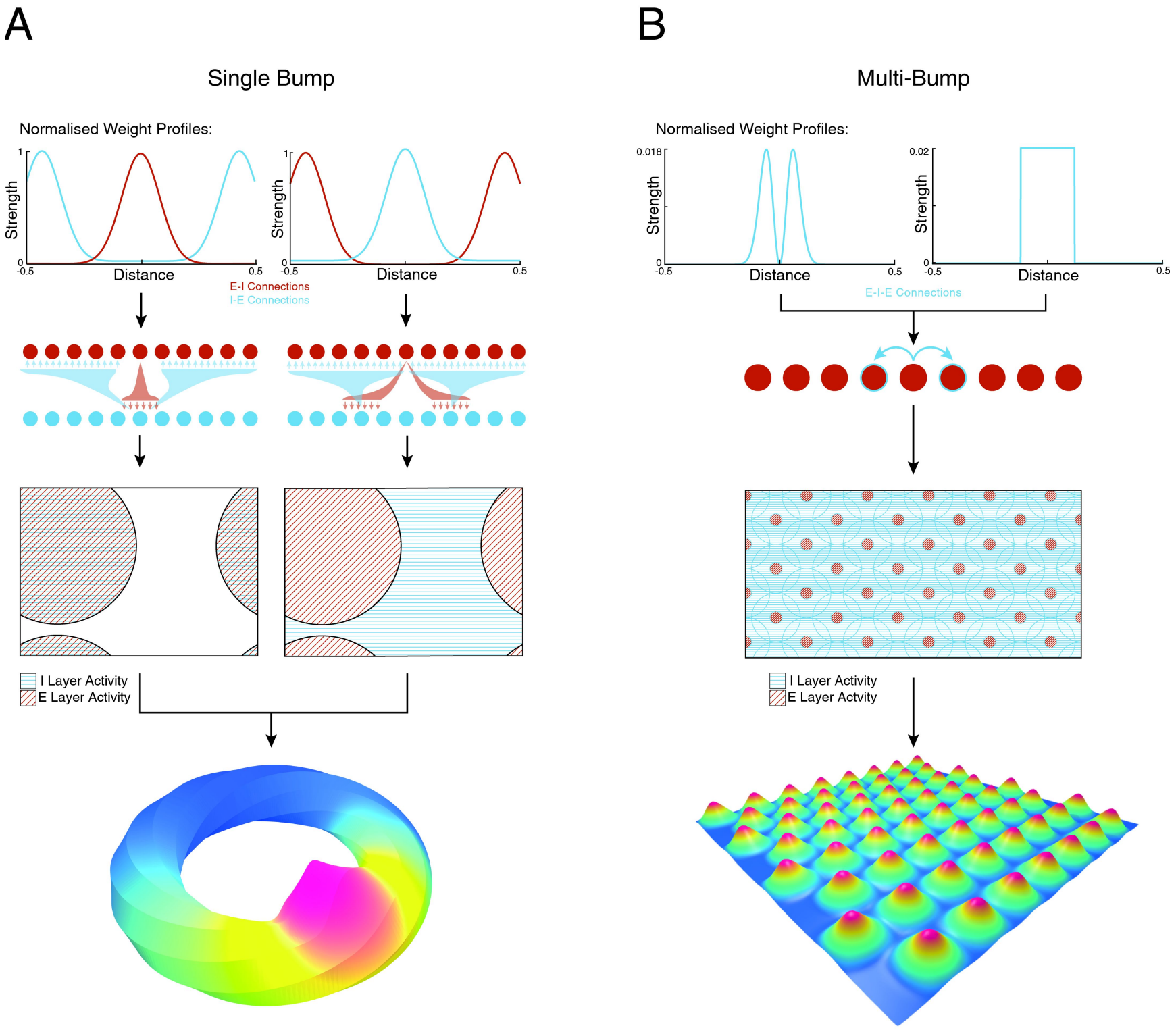
A
Single Bump
Normalised Weight Profiles:
Strength
1
0
-0.5
Distance
0.5
E-I Connections
I-E Connections
I Layer Activity
E Layer Activity
B
Multi-Bump
Normalised Weight Profiles:
0.018
0.02
E-I-E Connections
I Layer Activity
E Layer Actvity

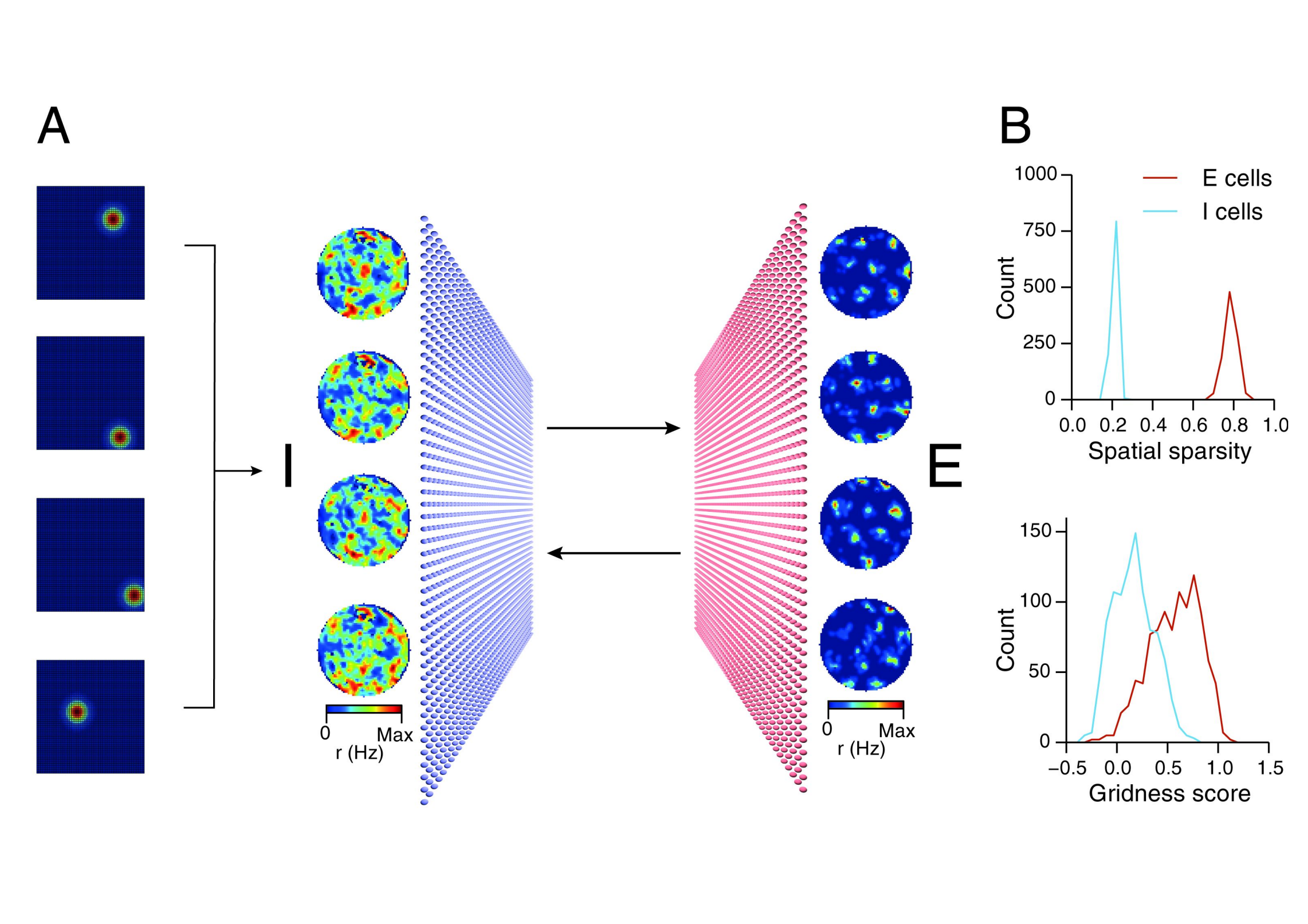
A
I
E
0
Max
r (Hz)
0
Max
r (Hz)
B
1000
750
500
250
0
Count
E cells
I cells
0.0
0.2
0.4
0.6
0.8
1.0
Spatial sparsity
150
100
50
0
Count
−0.5
0.0
0.5
1.0
1.5
Gridness score

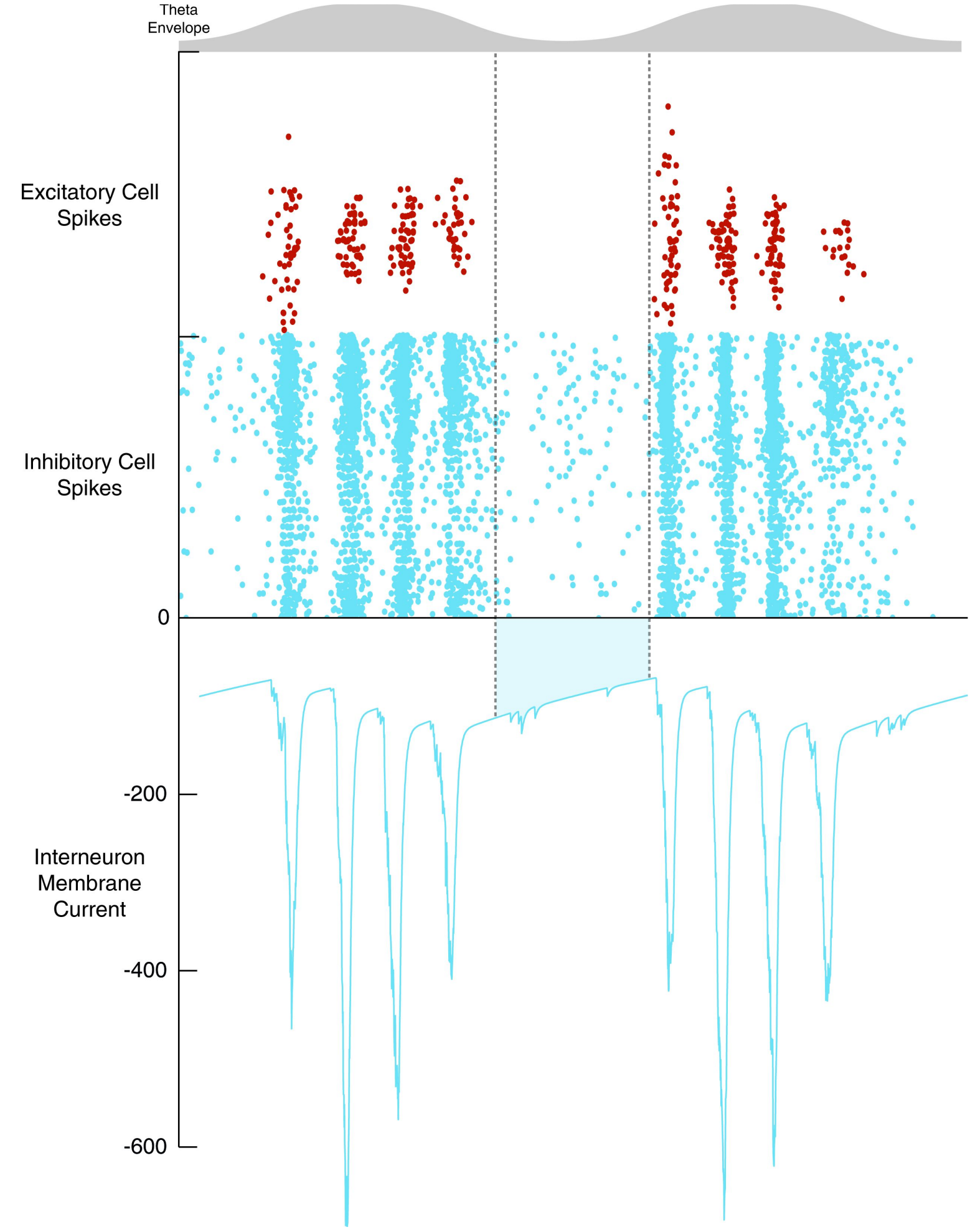
Theta
Envelope
Excitatory Cell
Spikes
Inhibitory Cell
Spikes
0
-200
Interneuron
Membrane
Current
-400
-600